

## Charge Transfer State Versus Hot Exciton Dissociation in Polymer–Fullerene Blended Solar Cells

Jiye Lee,<sup>†,‡</sup> Koen Vandewal,<sup>†,§</sup> Shane R. Yost,<sup>#</sup> Matthias E. Bahlke,<sup>‡</sup> Ludwig Goris,<sup>§</sup>  
Marc A. Baldo,<sup>\*,‡</sup> Jean V. Manca,<sup>\*,§</sup> and Troy Van Voorhis<sup>\*,#</sup>

*Department of Electrical Engineering and Computer Science, Massachusetts Institute of Technology, Cambridge, Massachusetts 02139, IMEC-IMOMEC, vzw and Institute for Materials Research, Hasselt University, Wetenschapspark 1, 3590 Diepenbeek, Belgium, and Department of Chemistry, Massachusetts Institute of Technology, Cambridge, Massachusetts 02139*

Received May 26, 2010; E-mail: baldo@mit.edu; jean.manca@uhasselt.be; tvan@mit.edu

**Abstract:** We examine the significance of hot exciton dissociation in two archetypical polymer–fullerene blend solar cells. Rather than evolving through a bound charge transfer state, hot processes are proposed to convert excitons directly into free charges. But we find that the internal quantum yields of carrier photogeneration are similar for both excitons and direct excitation of charge transfer states. The internal quantum yield, together with the temperature dependence of the current–voltage characteristics, is consistent with negligible impact from hot exciton dissociation.

The conversion of excitons into charge within organic solar cells is complicated by the uncertain role of bound electron–hole pairs, or charge transfer (CT) states at donor–acceptor interfaces.<sup>1–3</sup> In this communication, we perform direct photocurrent spectroscopy on CT states within organic solar cells. Our techniques allow us to decisively conclude that bound CT states mediate the conversion of excitons into charge. In contrast with expectations,<sup>1,4–7</sup> we find that charge generation is efficient despite the absence of ‘hot’ dissociation of excitons directly into charge. These findings confirm prior suggestions<sup>2,3,8</sup> that the photocurrent generation in organic solar cells is controlled by the recombination dynamics of thermally relaxed CT states.

Spectroscopy by Muntwiler et al. has determined that the binding energy of CT states is typically well in excess of 0.1 eV.<sup>1,4</sup> However, modern organic solar cells exhibit near-unity quantum yield, demonstrating that charge is efficiently generated despite the large binding energy of the CT state.<sup>9</sup> To resolve this possible conflict, a hot process of charge transfer has been proposed, whereby the excess energy from exciton dissociation,  $\Delta E_{CT} = E_X - E_{CT}$ , contributes to the dissociation of CT states. Here,  $E_X$  and  $E_{CT}$  are the energies of the exciton and CT states, respectively. In support of this model, it was observed that the population of free charge carriers increases as  $\Delta E_{CT}$  gets larger,<sup>5,6</sup> and Pensack et al. showed that the rate of free carrier formation is temperature-independent, implying that charge separation is barrierless.<sup>7</sup>

In this communication, we investigate the significance of hot exciton dissociation processes by comparing CT states generated from either excitons or direct photoexcitation. This approach is feasible because mixtures of polymers (donors) and fullerene molecules (acceptors) exhibit a new absorption band at infrared wavelengths. This broad absorption band is attributed to the

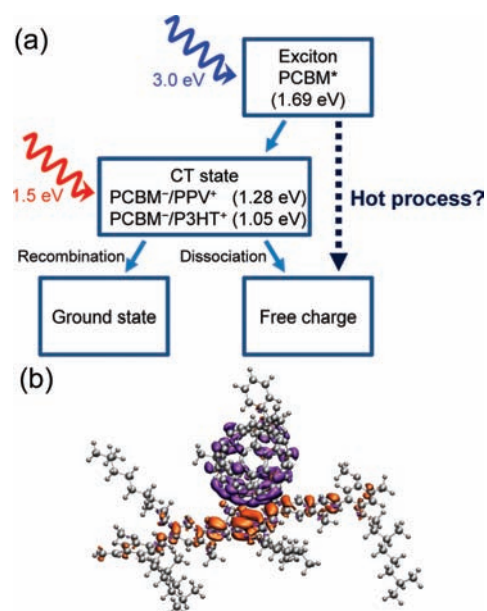


**Figure 1.** (a) Hot exciton dissociation processes are probed by comparing the output of solar cells under direct photoexcitation of either excitons or CT states. In a hot dissociation process, a donor or acceptor exciton breaks directly into free charge carriers without populating a bound, relaxed CT state. Alternatively, direct photoexcitation of CT states creates these bound CT states. The energy levels of excitons on PCBM molecules and CT states at the MDMO-PPV (P3HT)/PCBM interface are determined from the luminescence spectra.<sup>13</sup> (b) The calculated charge-density difference between the CT state and the ground state of an MDMO-PPV/PCBM heterodimer. The violet (orange) surfaces show where the CT state has more (less) electron density. In each picture PCBM is constrained to have an extra electron and a 5-unit MDMO-PPV is constrained to have a hole. The corresponding figure for a P3HT/PCBM pair is presented in the Supporting Information.

formation of bound CT states, mediated by the interaction of the highest occupied molecular orbital (HOMO) of donors with the lowest unoccupied molecular orbital (LUMO) of acceptors.<sup>10–12</sup> Thus, one can create thermally relaxed CT states by optically exciting the CT transition band directly.

As shown in Figure 1, CT states are excited directly and indirectly by below-gap and above-gap illumination, respectively. The existence of a hot CT process should yield observable differences in free carrier generation. First, we compare the internal quantum efficiency of directly excited CT states and CT states generated from excitons. Second, we measure the open-circuit voltage ( $V_{OC}$ ), a key charge recombination metric, under below-gap and above-gap illuminations with equivalent CT state generation

<sup>†</sup> These authors contributed equally.

<sup>‡</sup> Dept. of EECS, MIT.

<sup>§</sup> Hasselt University.

<sup>#</sup> Dept. of Chemistry, MIT.

rates. We also evaluate the temperature dependence of photocurrent for those two excitations.

We study two archetypal photovoltaic systems: bulk heterojunctions of poly[2-methoxy-5-(3',7'-dimethyloctyloxy)-1,4-phenylenevinylene] (MDMO-PPV) and poly-3(hexylthiophene) (P3HT) mixed with 1-(3-methoxycarbonyl)-propyl-1-phenyl-[6,6]C61 (PCBM). Goris et al.<sup>14,15</sup> and Vandewal et al.<sup>11</sup> previously demonstrated weak absorption and photocurrent generation from CT states in these heterojunctions. Time-resolved transient absorption spectroscopy by Drori et al. on polymer–fullerene blends has shown that below-gap excitation efficiently produces polarons on the polymer chains and fullerene molecules.<sup>16</sup>

The existence of below-gap CT states in these blends is supported by constrained density functional calculations.<sup>17</sup> As detailed in the Supporting Information, several MDMO-PPV/PCBM and P3HT/PCBM heterodimers were simulated with various intermolecular orientations. The surrounding molecules were assumed to provide a uniform dielectric surrounding the pair with  $\epsilon = 4$ . The resulting CT states were bound by 0–0.4 eV for MDMO-PPV/PCBM and 0–0.5 eV for P3HT/PCBM. The HOMO–LUMO band offset at the interface was 1.6 eV (1.6 eV) for MDMO-PPV/PCBM (P3HT/PCBM) suggesting CT absorption should be active at 1.2–1.6 eV for MDMO-PPV/PCBM and 1.1–1.6 eV for P3HT/PCBM. The calculated CT energies may be red-shifted because the density functional calculation overdelocalizes the electrons and, consequently, underpredicts the ionization potential of the polymers significantly.<sup>18</sup> The predicted CT energies are in agreement with the optical characterization by Goris et al.<sup>14,15</sup> and Vandewal et al.<sup>11</sup>

The spectral quantum efficiency and the absorption coefficient of organic layers were measured with a high sensitivity using Fourier-transform photocurrent spectroscopy (FTPS) and photo-thermal deflection spectroscopy (PDS), respectively, as described in refs 11 and 14. PDS was performed on ~200 nm-thick MDMO-PPV:PCBM and ~250 nm-thick P3HT:PCBM films on quartz substrates. FTPS was carried out on devices prepared with the same film thickness, sandwiched between indium tin oxide (ITO)/poly(3,4-ethylenedioxythiophene):poly(4-styrenesulphonate) (PEDOT:PSS) and Ca/Al electrodes.

Figure 2 shows the external quantum efficiency (EQE) at short-circuit conditions compared with the optical absorption of blends of MDMO-PPV:PCBM (1:4 by weight) and P3HT:PCBM (1:1 by weight). The absorption coefficients of each component in the blends are also shown. The weak absorption under 1.6 eV, observed for mixtures of the polymer and PCBM, is attributed to CT absorption.<sup>11,12</sup> The lowest energy part of the absorption spectra, below 1.4 and 1.2 eV for MDMO-PPV:PCBM and P3HT:PCBM systems, respectively, can be attributed to light- and aging-induced features and not CT transitions, as the absorption in this region increases upon repeating measurements on the same film; see Supporting Figure 3.

We fitted the EQE spectrum calculating the absorption of organic layers, i.e.,  $A_0 = A_0(1 - \exp(-2\alpha \cdot d))$ , where  $A_0$  accounts for the loss from ITO and PEDOT:PSS layers and is assumed to be 0.85,  $\alpha$  is the absorption coefficient measured with PDS, and  $d$  is the thickness of the blended films. Consequently, we obtained internal quantum efficiencies (IQEs) of  $(45 \pm 10)\%$  and  $(80 \pm 10)\%$  for MDMO-PPV:PCBM and P3HT:PCBM devices, respectively; see Supporting Figure 6 for the IQE as a function of energy. The fit, constant across the full wavelength range from above to below the optical gap, strongly suggests that the energies of excited CT states do not greatly influence CT state dissociation. Every optically accessible exciton and CT state exhibits a similar probability of charge generation or recombination. Even if our below-gap optical

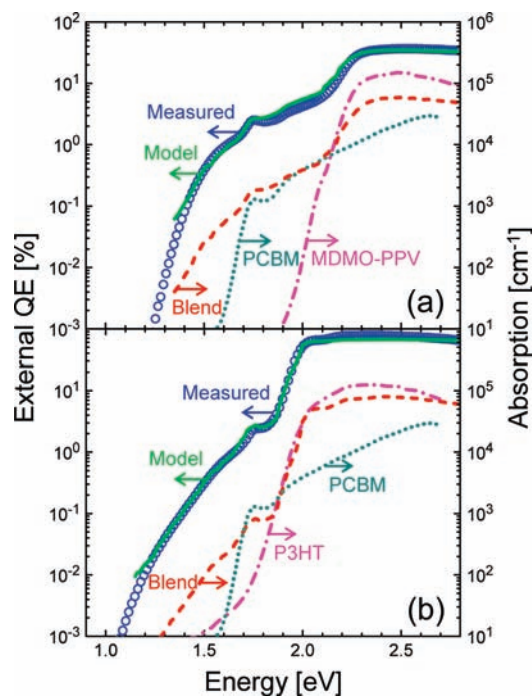


**Figure 2.** (a) The external quantum efficiency (EQE) spectrum (circles) under short-circuit conditions compared to the absorption spectrum of an MDMO-PPV:PCBM device. The absorption coefficients of MDMO-PPV (dash-dotted line), PCBM (dotted line), and blends (dashed line) are shown. The EQE was fit using IQEs of  $(45 \pm 10)\%$ . (b) The EQE spectrum (circles) and absorption spectrum of a P3HT:PCBM device. An IQE of  $(80 \pm 10)\%$  was obtained. For both heterojunctions, the CT state absorption band exhibits a charge collection efficiency similar to that of the polymer or PCBM.

excitation generates hot CT states, we find no change in the efficiency of charge generation despite varying the below-gap excitation energy by several tenths of an eV.

Figure 3 compares  $V_{OC}$  and photocurrents under below-gap and above-gap excitations at varying temperatures. Diode lasers with photon energies of 3.0 and 1.5 eV were used as light sources. Details of the device structure, fabrication, and characterizations are described in the Supporting Information. In order to equalize the initial CT generation rate for both excitations, the incident light intensity was adjusted using optical density filters to obtain a short-circuit current density of  $J = 32 \mu\text{A}/\text{cm}^2$  (for MDMO-PPV:PCBM) or  $J = 0.11 \text{ mA}/\text{cm}^2$  (for P3HT:PCBM) at 280 K for both laser wavelengths. For both heterojunctions, the photocurrent density decreased by more than an order of magnitude when the temperature was reduced from room temperature to below 50 K; see Supporting Figure 4.

$V_{OC}$  is a key indicator for charge recombination in organic solar cells and is logarithmically proportional to the photocurrent under the electric field at open-circuit conditions.<sup>19,20</sup> In both heterojunctions, we cannot resolve a difference in  $V_{OC}$  for temperatures above 130 K when CT states are excited rather than donor or acceptor excitons. But  $V_{OC}$  is  $(30 \pm 5)$  mV higher for above-gap excitation in MDMO-PPV:PCBM devices at temperatures below 130 K. The initial CT generation rates are not expected to change with temperature since the exciton diffusion yield in bulk heterojunctions is close to unity and hardly dependent on temperature.<sup>21</sup> Indeed, under reverse bias at  $V = -1$  V, we observe similar photocurrent densities for above-gap and below-gap excitations; see Figure 3b and 3d. Therefore, the slightly higher  $V_{OC}$  for above-gap excitations might mean that a hot CT process reduces the CT recombination loss by dissociating hot CT states before they collapse into deeper Coulomb potential wells. The effect is weak and only observable

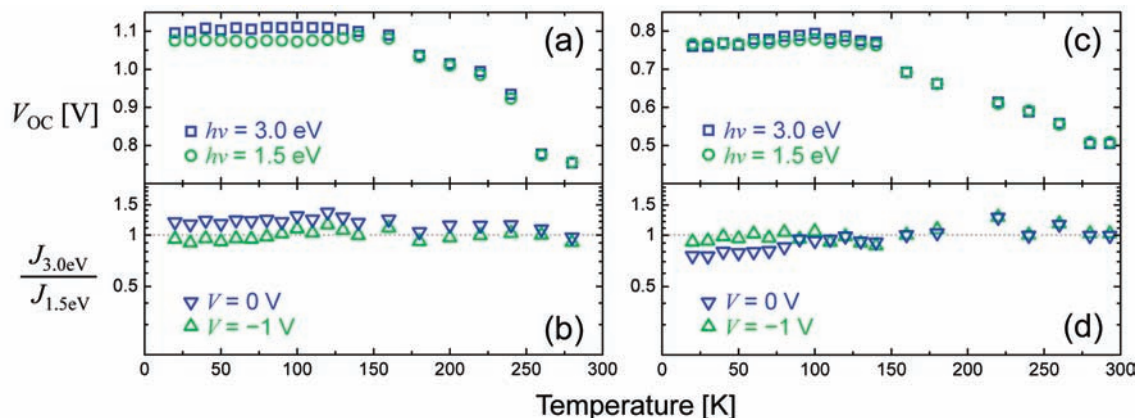


**Figure 3.** (a) Open-circuit voltage of an MDMO-PPV:PCBM device as a function of temperature under above-gap ( $h\nu = 3.0$  eV, squares) and below-gap ( $h\nu = 1.5$  eV, circles) excitations (b) Photocurrent ratio of above-gap and below-gap excitations at a voltage of  $V = 0$  V ( $\nabla$ ) and  $V = -1$  V ( $\Delta$ ). Equivalent of (a) and (b) for a P3HT:PCBM device, respectively.

at low temperature, perhaps because the relaxation of hot CT states slows down with decreasing phonon densities.

It is also notable in Figure 3b and 3d that the above-gap and below-gap excitations show the same temperature dependence of photocurrent. Under the concept of thermally assisted charge separation ( $J \approx \exp(-E_B/kT)$ , where  $E_B$  is the binding energy),<sup>2</sup> this implies that the binding energy of CT states created from exciton dissociation is equal to that of directly photogenerated bound CT states. We confirm this conclusion again by observing that below-gap and above-gap excitations generate the equivalent photocurrent under varying electric field; see Supporting Figure 5.

To summarize, we observe evidence at low temperatures that may be tentatively attributed to weak hot CT state phenomena. At temperatures close to room temperature, where solar cells usually operate, we find that the CT states formed from exciton splitting are indistinguishable from bound CT states.

Our photocurrent and voltage measurement results provide direct confirmation in solar cells of prior spectroscopic studies on above-gap and below-gap excitations. In optical pump–probe spectroscopy on P3HT or MEH-PPV blended with PCBM, both above-gap and below-gap excitations yielded similar carrier dynamics.<sup>22–24</sup> These studies, however, use below-gap pump wavelengths that excite the high energy part of the CT band. By varying the excitation wavelengths through the CT band we show that it is the thermally relaxed CT states, not hot CT states, which mediate the conversion between excitons and free charge carriers.

We also extend prior electrical studies on the CT states. Zhou et al. reported that a modest quantum yield of photocurrent is produced even when the driving force for exciton dissociation  $\Delta E_{CT}$  is only  $\sim 100$  meV.<sup>8</sup> Additionally, it has been shown that the electric-field-induced quenching of CT emission matches the field dependence of photocurrent, meaning that it is the thermally relaxed, light-emitting CT state that is formed right before charge separation.<sup>3,8</sup>

Our results imply that excess exciton energies at the donor–acceptor interface are not required for efficient photocurrent generation, at least at room temperature. The absence of hot exciton dissociation processes is expected to be especially significant for the  $V_{OC}$  of low-energy gap organic solar cells because the necessity for a large  $\Delta E_{CT}$  might otherwise dissipate a substantial fraction of the potential open-circuit voltage.<sup>12,20</sup>

**Acknowledgment.** Work at MIT and Hasselt University was supported by the U.S. Department of Energy (Award No. DE-FG02-07ER46474) and the Institute for the Promotion of Science and

Technology in Flanders, respectively. J.L. thanks the Korea Foundation for Advanced Studies for a graduate fellowship.

**Supporting Information Available:** Constrained density functional calculations, absorption spectra upon repeated measurements, details of the experimental method, electric-field and temperature dependence of photocurrent. This material is available free of charge via the Internet at <http://pubs.acs.org>.

## References

- Zhu, X. Y.; Yang, Q.; Muntwiler, M. *Acc. Chem. Res.* **2009**, *42*, 1779.
- Blom, P. W. M.; Mihailescu, V. D.; Koster, L. J. A.; Markov, D. E. *Adv. Mater.* **2007**, *19*, 1551.
- Veldman, D.; Ipek, O. z.; Meskers, S. C. J.; Sweelssen, J. r.; Koetse, M. M.; Veenstra, S. C.; Kroon, J. M.; Bavel, S. S. v.; Loos, J.; Janssen, R. A. J. *J. Am. Chem. Soc.* **2008**, *130*, 7721.
- Muntwiler, M.; Yang, Q.; Tisdale, W. A.; Zhu, X. Y. *Phys. Rev. Lett.* **2008**, *101*, 196403.
- Ohkita, H.; Cook, S.; Astuti, Y.; Duffy, W.; Tierney, S.; Zhang, W.; Heeney, M.; McCulloch, I.; Nelson, J.; Bradley, D. D. C.; Durrant, J. R. *J. Am. Chem. Soc.* **2008**, *130*, 3030.
- Clarke, T. M.; Ballantyne, A. M.; Nelson, J.; Bradley, D. D. C.; Durrant, J. R. *Adv. Funct. Mater.* **2008**, *18*, 4029.
- Pensack, R. D.; Asbury, J. B. *J. Am. Chem. Soc.* **2009**, *131*, 15986.
- Zhou, Y.; Tvingstedt, K.; Zhang, F.; Du, C.; Ni, W.-X.; Andersson, M. R.; Inganäs, O. *Adv. Funct. Mater.* **2009**, *19*, 3293.
- Park, S. H.; Roy, A.; Beaupre, S.; Cho, S.; Coates, N.; Moon, J. S.; Moses, D.; Leclerc, M.; Lee, K.; Heeger, A. J. *Nat. Photonics* **2009**, *3*, 297.
- Benson-Smith, J. J.; Goris, L.; Vandewal, K.; Haenen, K.; Manca, J. V.; Vanderzande, D.; Bradley, D. D. C.; Nelson, J. *Adv. Funct. Mater.* **2007**, *17*, 451.
- Vandewal, K.; Gadisa, A.; Oosterbaan, W. D.; Bertho, S.; Banishoeib, F.; Van Severen, I.; Lutsen, L.; Cleij, T. J.; Vanderzande, D.; Manca, J. V. *Adv. Funct. Mater.* **2008**, *18*, 2064.
- Vandewal, K.; Tvingstedt, K.; Gadisa, A.; Inganäs, O.; Manca, J. V. *Nat. Mater.* **2009**, *8*, 904.
- Tvingstedt, K.; Vandewal, K.; Gadisa, A.; Zhang, F. L.; Manca, J.; Inganäs, O. *J. Am. Chem. Soc.* **2009**, *131*, 11819.
- Goris, L.; Haenen, K.; Nesladek, M.; Wagner, P.; Vanderzande, D.; De Schepper, L.; D'Haen, J.; Lutsen, L.; Manca, J. V. *J. Mater. Sci.* **2005**, *40*, 1413.
- Goris, L.; Poruba, A.; Hod'akova, L.; Vanecek, M.; Haenen, K.; Nesladek, M.; Wagner, P.; Vanderzande, D.; De Schepper, L.; Manca, J. V. *Appl. Phys. Lett.* **2006**, *88*, 052113.
- Drori, T.; Sheng, C. X.; Ndobe, A.; Singh, S.; Holt, J.; Vardeny, Z. V. *Phys. Rev. Lett.* **2008**, *101*, 037401.
- Wu, Q.; Van Voorhis, T. J. *Phys. Chem. A* **2006**, *110*, 9212.
- Cohen, A. J.; Mori-Sanchez, P.; Yang, W. *Science* **2008**, *321*, 792.
- Vandewal, K.; Tvingstedt, K.; Gadisa, A.; Inganäs, O.; Manca, J. V. *Phys. Rev. B* **2010**, *81*, 125204.
- Rand, B. P.; Burk, D. P.; Forrest, S. R. *Phys. Rev. B* **2007**, *75*, 115327.
- Mikhnenko, O. V.; Cordella, F.; Sieval, A. B.; Hummelen, J. C.; Blom, P. W. M.; Loi, M. A. J. *Phys. Chem. B* **2008**, *112*, 11601.
- Cunningham, P. D.; Hayden, L. M. *J. Phys. Chem. C* **2008**, *112*, 7928.
- Parkinson, P.; Lloyd-Hughes, J.; Johnston, M. B.; Herz, L. M. *Phys. Rev. B* **2008**, *78*, 115321.
- Bakulin, A. A.; Martynov, D.; Paraschuk, D. Y.; Loosdrecht, P. H. M. v.; Pshenichnikov, M. S. *Chem. Phys. Lett.* **2009**, *482*, 99.

JA1045742